Experimental analysis of photovoltaic cogeneration modules

F. Busato, R. Lazzarin, and M. Noro (corresponding author)
Department of Management & Engineering – University of Padova – Stradella S. Nicola, 3 – 36100 Vicenza – ITALY
E-mail: marco.noro@unipd.it

Abstract PhotoVoltaic/Thermal cogeneration (PV/T) technology seems to offer very interesting prospects, also considering recent economic incentives on renewable energies issued in Italy. Conversely, some problems have to be faced: good thermal behaviour of the module studying the best thermal exchange between the solar cells and the channelled plate below, selection of the best working temperature according to the need of the plant served by the solar modules, and selection of the best fluid to remove heat.

This paper reports on the first results of a survey on electrical and thermal efficiency of some PV/T prototypes, carried out at the experimental testing rig built in Vicenza, varying some parameters (solar radiation, water flow, inlet water temperature). Experimental measurements show very different results for the three PV/T collectors tested. For a particular collector a simulation model has been developed, based on a detailed analytical model, and simulated results have been compared to experimental results.

Keywords cogeneration; photovoltaic; solar energy; renewable energy

Nomenclature

Symbol	
A_{coll}	collector aperture area, m^2
c_p	specific heat, kJ kg^{-1} K^{-1}
D_{eq}	equivalent hydraulic diameter, m
$E_{electrical}$	solar radiation quota converted into electrical energy, W m^{-2}
h_{in}	inlet fluid enthalpy, kJ kg^{-1}
h_{out}	outlet fluid enthalpy, kJ kg^{-1}
I	collector PV current, A
$\dot{m}$	fluid specific mass flow rate, kg s^{-1} m^{-2}
q	useful thermal power, kW
q_{ex}	exergy of q, kW
q_{fin}	heat transferred in the absorber, kW
q_{fluid}	total heat gained by the fluid, kW
$Q_{heat,abs}$	solar radiation quota absorbed by the absorber, W m^{-2}
$Q_{heat,conv}$	solar radiation quota wasted by convection with ambient air, W m^{-2}
$Q_{heat,rad}$	solar radiation quota wasted by radiation with the sky, W m^{-2}
R_{back}	thermal resistance between absorber and rear collector layer, W m^{-2} K^{-1}
S	global solar radiation, W m^{-2}
s_{abs}	absorber thickness, m
s_{cover}	glazing thickness, m
s_{in}	inlet fluid entropy, kJ kg^{-1} K^{-1}

s_{out} outlet fluid entropy, kJ kg^{-1} K^{-1}
T_{abs} absorber temperature, ºC
T_{amb} ambient temperature, ºC
T_{avg} average fluid temperature, ºC
T_{base} base temperature, ºC
$T_{cover,down}$ glazing lower surface temperature, ºC
$T_{cover,up}$ glazing upper surface temperature, ºC
T_{in} inlet fluid temperature, ºC
T_c photovoltaic cells layer temperature, ºC
T_{out} outlet fluid temperature, ºC
T_r reference temperature, ºC
T_{red} reduced temperature, m^2 K W^{-1}
V collector PV voltage, V

Greek symbol

$\alpha_{gap,conv}$ convection coefficient with the gap gas, W m^{-2} K^{-1}
$\alpha_{gap,rad}$ radiation coefficient with the gap gas, W m^{-2} K^{-1}
$\alpha_{sky,conv}$ convection coefficient with the sky, W m^{-2} $^{-1}$
$\alpha_{sky,rad}$ radiation coefficient with the sky, W m^{-2} K^{-1}
β temperature coefficient, ºC $\%^{-1}$
ε_{cover} glazing emissivity
ε_{PV} photovoltaic cells layer emissivity
η_e electrical efficiency
η_r nominal electrical efficiency (at reference temperature T_r)
η_t thermal efficiency
$\eta_{ex,t}$ exergetic quota of the useful thermal power
λ_{abs} absorber conductivity, J m^{-1} K^{-1}
λ_{cover} glazing conductivity, J m^{-1} K^{-1}
$\tau\alpha$ transmission-absorption product
σ Stefan-Boltzmann constant, W m^{-2} K^{-4}
$\xi_{ex,e}$ electrical exergetic efficiency
$\xi_{ex,t}$ thermal exergetic efficiency
$\xi_{ex,tot}$ total exergetic efficiency

1. Introduction

The weather conditions of Italy, with a good level of insolation, should encourage more development of renewable energies, especially those coming from the direct usage of sun, like photovoltaics and solar thermal collectors. That awareness together with Kyoto protocol constraints has led the Italian government to introduce new grant systems [1], [2], [3], and [4]. This favourable scenario is then also interesting for the application of photovoltaic-thermal (PV/T) systems. The main idea is to increase the electrical production of PV by decreasing the normal operating cell temperature by cooling the panel with water (or air), but also to have higher global

efficiency with an enhanced use of solar energy. So PV/T aims to utilise the same area both for producing electricity and heat.

The photovoltaic-thermal technology has been studied since the 1970s when the energy crisis gave increase to the development of alternative ways of producing energy to that of fossil fuels. The different types of photovoltaic cogeneration (ventilated PV, daylighting, PV/T) are well described in [5], [6], and [7]. The more common PV/T technology, the flat plate collector, is the object of the present analysis.

2. Flat plate PV/T collector

The main four types of flat plate collector (Figure 1) differ from each other in function of the fluid used to remove heat (liquid or air) and of the use of a glass cover to lower the frontal panel heat losses (glazed or unglazed).

The purpose of the technology is to collect the heat released by the PV laminate surface (which is not able to completely convert all the global solar radiation to electrical energy) as much as it can, putting in close contact the laminate rear part and the thermal absorber, typically made in copper or aluminium, using special glues or similar compounds. Therefore, heat is exchanged to a fluid (water, mixture of water and anti-freezing liquid or air) flowing into channels or pipes as parts of the absorber. Thermal losses are kept low by using a suitable insulation on the edges and the bottom part of the collector. There are two main critical points:

– the contact between the rear part of the cells and the thermal absorber has to be enhanced to reduce the thermal resistances both of conduction and interface among the different layers: PV laminate, glue, metal absorber. That is much more relevant when considering an unglazed collector which has large frontal heat

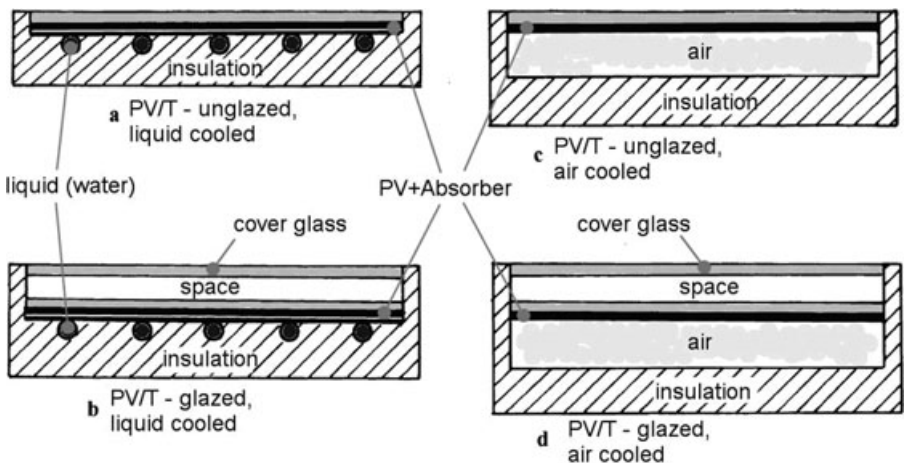

Figure 1. *PV/T flat plate collector: liquid cooled (a,b) and air cooled (c,d) with and without glass cover.*

dissipation due to the lack of the additional insulation of the glass cover. The suggested compounds used to glue the PV and the absorber should be highly conductive and of reduced section: films of silicon rubbers with inclusions of conductive material (λ = 1 W m^{-1} K^{-1}), epoxy glues (λ = 3 W m^{-1} K^{-1}), ultra-conductive film (λ up to 15 W m^{-1} K^{-1}).
– the glass cover in the glazed type is beneficial to limit the frontal thermal losses but this positive effect has a main drawback due to the risk of delamination of the PV cells as a consequence of the high stagnation temperatures. Indeed, during hot periods and when the user is not asking for heat, the collector is not supposed to be cooled anymore: that results in an increase of the cells temperature up to 150ºC when the PV panels in the worst conditions are said to raise up to 80ºC. Therefore it is necessary to provide a safety system to prevent the PV/T module reaching such high stagnation temperatures (that could be a valve that opens the water circuit when the water temperature inside the tank rises up to a fixed set point).

There are some relevant advantages for using PV/T systems:

– the surface required is around half the one needed by the PV and solar thermal collectors for producing the same amount of energy. That is quite interesting when considering buildings with small roofs compared to the dwellings (flats) of highly populated areas (like Japan);
– the reduction in the costs of common parts like frames, holding structures, glasses, documentation, installation and so on;
– enhanced utilization of the solar energy if compared to a PV collector (the efficiency is the sum of the electrical and thermal yields);
– the increased cells electrical efficiency when suitable low temperature applications are available, allowing the collector to work at lower temperatures than for a PV collector;
– better architectural building integration due to the uniform appearance compared to the two separated systems;
– the possibility to have access to more government incentives for both PV and solar thermal.

3. PV/T collector model and simulations

A simulation model of the COGEN PV/T collector (see next section 4) has been developed in order to predict the performance in steady state conditions by varying numerous parameters (such as fluid flow rate, fluid temperature inlet, etc). The collector has been divided into elementary volumes individually solved, considering heat transmission in the z direction only (Figure 2). Each elementary volume contains:

– 4 mm thick tempered glazing to obtain a 20 mm gap interspace;
– Photovoltaic laminate composed by Tedlar, EVA, silicon cells, EVA;

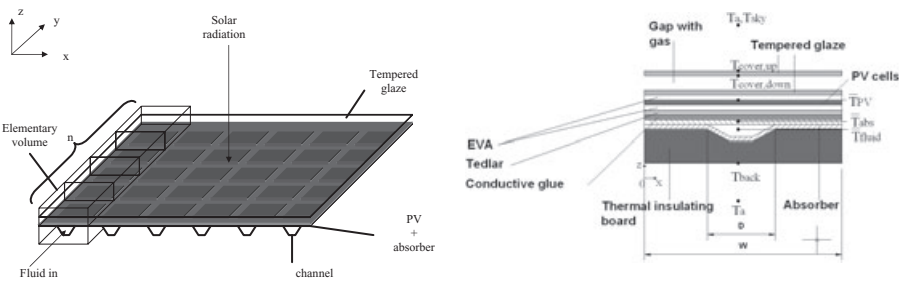

Figure 2. *Elementary volumes (left) and temperature positions (right) of the PV/T collector.*

– Conductive glue;
– Absorber;
– Thermal insulating board.

Boundary conditions are the following parameters:

– S (global solar radiation, W m^{-2});
– v (wind velocity, m s^{-1});
– T_{amb} (ambient temperature, ºC);
– T_{in} (inlet fluid temperature, ºC);

in addition to the following geometric characteristics of the PV/T module:

– length and width, m;
– thickness of the various layers, m;
– pipes size (length and cross section area).

The model calculates the temperatures of the various layers from a first attempt value of the mean photovoltaic laminate temperature T_{PV}, with inlet water temperature, outdoor air and sky temperatures as input values.

The starting point is the first law of thermodynamics applied to the collector (Equation 1):

$$S^* - E_{elctrical} - Q_{heat,abs} - Q_{loss,conv} - Q_{loss,rad} = 0 \tag{1}$$

Consider the following obvious Equation 2 and Equation 3:

$$S^* = (\tau\alpha)S \tag{2}$$

$$E_{electrical} = (\tau\alpha)\eta_e S \tag{3}$$

with $\tau\alpha$ the transmission-absorption product and η_e the electrical efficiency, function of the PV cells temperature T_c (Equation 4):

$$\eta_e = \eta_r \cdot [1 - \beta(T_c - T_r)] \tag{4}$$

Heat transferred by conduction through the glazing equals heat wasted by radiation and convection (Equation 5):

$$\alpha_{sky,rad}\left(T_{cover,up} - T_{sky}\right) + \alpha_{sky,conv}\left(T_{cover,up} - T_{amb}\right) = \frac{\lambda_{cover}}{s_{cover}}\left(T_{cover,down} - T_{cover,up}\right) \tag{5}$$

In steady state, such thermal energy has to equal heat transferred by radiation (between the two internal gap surfaces) and by convection (with internal gap gas) (Equation 6):

$$\frac{\lambda_{cover}}{s_{cover}}\left(T_{cover,down} - T_{cover,up}\right) = \alpha_{gap,rad}\left(\overline{T}_{PV} - T_{cover,down}\right) + \alpha_{gap,conv}\left(\overline{T}_{PV} - T_{cover,down}\right) \tag{6}$$

Energy transferred by convection and radiation in the gap is equal to S^* minus electrical energy produced and heat transferred to the absorber (Equation 7):

$$\begin{aligned}&\alpha_{gap,rad}\left(\overline{T}_{PV} - T_{cover,down}\right) + \alpha_{gap,conv}\left(\overline{T}_{PV} - T_{cover,down}\right) = \\ &\quad S^* - E_{electrical} - \frac{\left(\overline{T}_{PV} - \overline{T}_{abs}\right)}{R_{tot}} = S' - \frac{\left(\overline{T}_{PV} - \overline{T}_{abs}\right)}{R_{tot}}\end{aligned} \tag{7}$$

$\alpha_{sky,rad}$ and $\alpha_{gap,rad}$ are coefficients expressed by (Equations 8 and 9):

$$\alpha_{sky,rad} = \varepsilon_{cover}\sigma\left(T_{cover,up} + T_{sky}\right)\left(T_{cover,up}^2 + T_{sky}^2\right) \tag{8}$$

$$\alpha_{gap,rad} = \varepsilon_{PV}\sigma\left(\overline{T}_{PV} + T_{cover,down}\right)\left(\overline{T}_{PV}^2 + T_{cover,down}^2\right) \tag{9}$$

Considering an elementary section dx in the x direction of the elementary volume, it is possible to write the following heat conduction equation (Equation 10):

$$\lambda_{abs} s_{abs} \frac{d^2 T_{abs}(x)}{dx^2} = \frac{\left(T_{abs}(x) - T_{back}(x)\right)}{R_{back}} - \frac{\left(T_{PV}(x) - T_{abs}(x)\right)}{R_{tot}} \tag{10}$$

Using Equation 1 and applying it to the elementary section dx we define the temperature profile in the x direction (Equation 11):

$$\begin{aligned}\frac{d^2 T_{abs}(x)}{dx^2} = \frac{C}{\lambda_{abs} s_{abs}}\Bigg[&T_{abs}(x)\left(\frac{1}{R_{tot}C} + \frac{1}{R_{back}C} - \frac{1}{R_{tot}}\right) - \\ &\left(S^* + \alpha_{gap,rad} T_{cover,down} + \alpha_{gap,conv} T_{cover,down} + \frac{T_{back}}{R_{back}C}\right)\Bigg]\end{aligned} \tag{11}$$

where:

$$C = \frac{1}{\alpha_{gap,rad} R_{tot} + \alpha_{gap,conv} R_{tot} + 1} \tag{12}$$

Equation 11 can be written as (Equation 13):

$$\frac{d^2\Theta}{dx^2} - m^2\Theta = 0 \tag{13}$$

where:

$$\Theta = T_{abs} - \frac{S' + \alpha_{gap,rad} T_{cover,down} + \alpha_{gap,conv} T_{cover,down} + \frac{T_{back}}{R_{back} C}}{\frac{1}{R_{tot} C} + \frac{1}{R_{back} C} - \frac{1}{R_{tot}}} \tag{14}$$

$$m = \sqrt{\frac{C\left(\frac{1}{R_{tot} C} + \frac{1}{R_{back} C} - \frac{1}{R_{tot}}\right)}{\lambda_{abs} s_{abs}}} \tag{15}$$

General solution of Equation 13 is (Equation 16):

$$\Theta = C_1 \sinh(mx) + C_2 \cosh(mx) \tag{16}$$

Because adjacent elementary volumes are adiabatic we have the condition (Equation 17):

$$\frac{d\Theta}{dx} = 0 \quad for\ x = 0 \tag{17}$$

If we let the fluid wet absorber temperature T_{abs} (that is for $x = \left(\frac{W - D_{tube}}{2}\right)$) be equal to the base temperature T_{base}, we have (Equation 18):

$$\Theta = T_{base} - \frac{S' + \alpha_{gap,rad} T_{cover,down} + \alpha_{gap,conv} T_{cover,down} + \frac{T_{back}}{R_{back} C}}{\frac{1}{R_{tot} C} + \frac{1}{R_{back} C} - \frac{1}{R_{tot}}} \quad per\ x = \left(\frac{W - D_{tube}}{2}\right) \tag{18}$$

Because of the boundary conditions, we calculate the two constants of Equation 16 (Equation 19):

$$C_1 = 0$$

$$C_2 = \frac{T_{base} - C_3}{\cosh\left(m\frac{W - D_{tube}}{2}\right)}$$

$$G_3 = \frac{S' + \alpha_{gap,rad}T_{cover,down} + \alpha_{gap,conv}T_{cover,down} + \frac{T_{back}}{R_{back}C}}{\frac{1}{R_{tot}C} + \frac{1}{R_{back}C} - \frac{1}{R_{tot}}} \tag{19}$$

Substituting the coefficients of Equation 16 we define the absorber temperature profile in the x direction (Equation 20):

$$T_{abs}(x) = C_3 + (T_{base} - C_3)\frac{\cosh(mx)}{\cosh\left(m\frac{W - D_{tube}}{2}\right)} \quad 0 < x < \frac{W - D_{tube}}{2} \tag{20}$$

Heat transferred in the absorber (from $x = 0$ to $x = \frac{W - D_{tube}}{2}$) is (Equation 21):

$$q_{fin} = -\lambda_{abs}s_{abs}\frac{dT_{abs}(x)}{dx} = \lambda_{abs}s_{abs}m(C_3 - T_{base})\tanh\left(m\frac{W - D_{tube}}{2}\right) \tag{21}$$

Considering that each elementary volume includes two absorber surfaces (left and right of each channel) and that the channel wall temperature is quite similar to the fluid wet absorber temperature, the total heat gained by the fluid is (Equation 22):

$$q_{fluid} = \left(\frac{T_{base} - \overline{T}_{fluido}}{\frac{1}{\alpha_{fluid}D_{tube}} + \frac{s_{abs}}{\lambda D_{tube}}}\right) = D_{tube}\left(\frac{T_{PV} - T_{base}}{R_{tot}}\right) - D_{tube}\left(\frac{T_{base} - T_{back}}{R_{back}}\right) + 2q_{fin} \tag{22}$$

Combining Equations 1, 21 and 22 we obtain (Equation 23):

$$q_{fluid} = \frac{k}{\theta}T_{fluid} + \frac{\varepsilon}{\theta} \tag{23}$$

where:

$$k = -D_{eq}C\left(\alpha_{gap,rad} + \alpha_{gap,conv} + \frac{T_{back}}{R_{back}C}\right) - 2\lambda_{abs}s_{abs}m\tanh\left(m\frac{W - D_{tube}}{2}\right) \quad (24)$$

$$\theta = 1 + \left(\frac{1}{\alpha_{fluid}D_{tube}} + \frac{s_{abs}}{\lambda D_{tube}}\right)\cdot \left[D_{eq}C\left(\alpha_{gap,rad} + \alpha_{gap,conv} + \frac{T_{back}}{R_{back}C}\right) + 2\lambda_{abs}s_{abs}m\tanh\left(m\frac{W - D_{tube}}{2}\right)\right] \quad (25)$$

$$\varepsilon = D_{eq}C\left(S' + \alpha_{sky,rad}T_{sky} + \alpha_{sky,conv}T_a + \frac{T_{back}}{R_{back}C}\right) + 2\lambda_{abs}s_{abs}m\tanh\left(m\frac{W - D_{tube}}{2}\right)\cdot C_3 \quad (26)$$

Equation 23 allows one to calculate the heat transferred by the absorber to the fluid in each elementary volume and at a given fluid temperature. In the *y* direction, temperature will change in function of exchanged thermal energy. So it is (Equation 27):

$$q_{fluid} = \frac{\dot{m}}{N}C_p\frac{dT_{fluid}}{dy} \quad (27)$$

where:
N is the total number of parallel channels.

By Equations 23 and 27 we obtain the variation of the fluid temperature in the *y* direction (Equation 28):

$$\frac{dT_{fluid}}{dy} = \frac{N}{\dot{m}C_p}\frac{k}{\theta}T_{fluid} + \frac{N}{\dot{m}C_p}\frac{\varepsilon}{\theta} \quad (28)$$

Integrating Equation 28 we obtain fluid temperature as a function of the position along the channel at a given inlet temperature $T_{fluid,in}$ (Equation 29):

$$T_{fluid}(y) = \left(T_{fluid,in} + \frac{\varepsilon}{k}\right)\exp\left(\frac{N}{\dot{m}C_p}\frac{k}{\theta}y\right) - \frac{\varepsilon}{k} \quad (29)$$

So, heat transferred to the fluid in the generic *i*-th elementary volume is (Equation 30):

$$Q_i = \frac{\dot{m}}{N} C_p \left(T^i_{fluid,out} - T^i_{fluid,in} \right) = \frac{\dot{m}}{N} C_p \left(T^i_{fluid,out} - T^{i-1}_{fluid,out} \right) \tag{30}$$

Integrating Equation 29 between the inlet and outlet of each elementary volume and dividing by the channel segment length we obtain the fluid mean temperature (Equation 31):

$$\bar{T}^i_{fluid} = \left(\frac{T^i_{fluid,in} + \frac{\varepsilon}{k}}{\frac{N}{\dot{m}C_p} \frac{k}{\theta} \frac{L}{n}} \right) \exp\left(\frac{N}{\dot{m}C_p} \frac{k}{\theta} \frac{L}{n} \right) - \left(\frac{T^i_{fluid,in} + \frac{\varepsilon}{k}}{\frac{N}{\dot{m}C_p} \frac{k}{\theta} \frac{L}{n}} \right) - \frac{\varepsilon}{k} \tag{31}$$

T_{base} can be now calculated using Equation 30 and 31 in the first part of Equation 22.

So now it has to be calculated, the absorber mean temperature as a weighted mean T_{base} and $\bar{T}_{fin}$ The latter is determined by integrating Equation 20 (Equation 32):

$$\bar{T}_{fin} = \frac{S' + \alpha_{gap,rad} T_{cover,down} + \alpha_{gap,conv} T_{cover,down} + \frac{T_{back}}{R_{back} C}}{\frac{1}{R_{tot} C} + \frac{1}{R_{back} C} - \frac{1}{R_{tot}}} + \frac{\left(T_{base} - \frac{S' + \alpha_{gap,rad} T_{cover,down} + \alpha_{gap,conv} T_{cover,down} + \frac{T_{back}}{R_{back} C}}{\frac{1}{R_{tot} C} + \frac{1}{R_{back} C} - \frac{1}{R_{tot}}} \right) \tanh\left(m \frac{W - D_{tube}}{2} \right)}{m \frac{W - D_{tube}}{2}} \tag{32}$$

So, the absorber mean temperature for each elementary volume is (Equation 33):

$$\bar{T}_{abs} = \frac{D_{tube} T_{base} + (W - D_{tube}) \bar{T}_{fin}}{W} \tag{33}$$

To solve all the equations cited the software does all the calculations in an iterative way from two initial values:

- initial values of the photovoltaic surface and the glazing internal surface temperatures;
- calculation of the electrical efficiency (Equation 4);

– calculation of the absorbed solar radiation (Equation 2) inclusive of the electrical energy quota (Equation 3);
– calculation of the glazing internal surface (Equations 5, 6 and 7): if calculated value is different from initial value, repeat 1–3 steps;
– calculation of the fluid outlet temperature for the *i*-th elementary volume (Equation 29);
– calculation of the heat exchanged with the fluid for the *i*-th elementary volume (Equation 30);
– calculation of the fluid wet absorber temperature for the *i*-th elementary volume (Equations 30, 31 and 22);
– calculation of the not fluid wet absorber temperature for the *i*-th elementary volume (Equation 32);
– calculation of the absorber mean temperature for the *i*-th elementary volume (Equation 33);
– calculation of the photovoltaic surface mean temperature (Equations 6 or 8): if this value is different from the initial value, repeat 1–9 steps.

Figure 3 reports the thermal and electrical efficiencies calculated by the software with the conditions similar to the real collector configuration. It is interesting to note that for the COGEN collector the calculated values are in good agreement with the measurements (see next section 4).

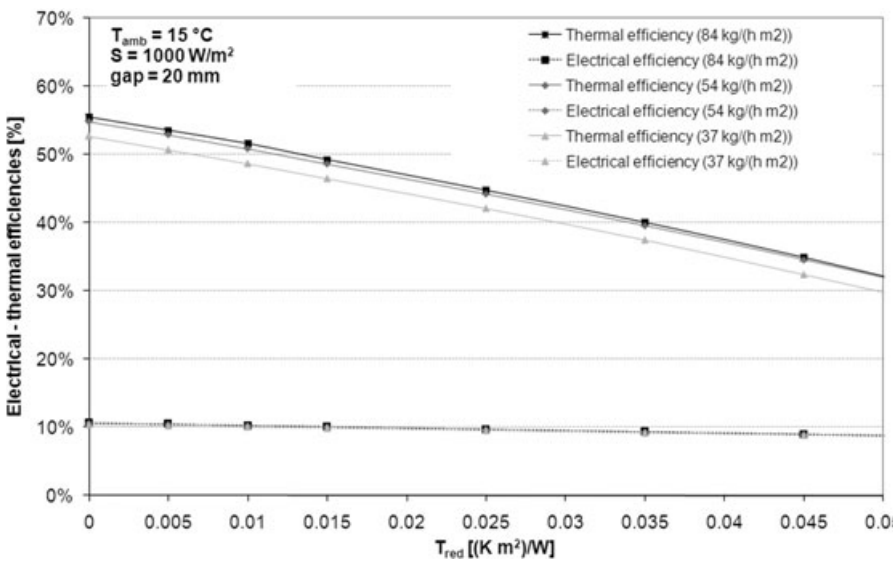

Figure 3. *Simulated electrical and thermal efficiencies comparison between three different fluid flow rate.*

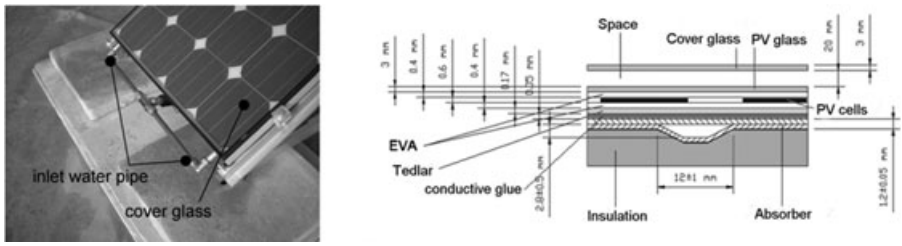

Figure 4. *COGEN: frontal view detail (left) and cross-section view (right).*

4. PV/T collectors and test rig arrangement

The PV/T test rig is set in Vicenza in the north-east of Italy on the flat roof of a building which is part of the Department of Industrial Management and Engineering (University of Padova). The aim is to test the performance of different collectors under the same test methods and boundary conditions. The collectors tested are:

- COGEN – It is a flat plate, glazed, liquid cooled collector, developed by the Department together with a private company. The cells are a single-crystalline type with a gross area of 1.2 m^2 (overall dimensions: 1.70 m × 1.20 m × 0.07 m) and nominal power of 135 W_p (open circuit voltage of 22.7 V, short circuit current of 8.45 A and electrical efficiency of 11.2% (without cover glass) at STC). The absorber is a roll-bond type made of aluminium and suitably glued to the Tedlar film of the PV laminate (thermal resistances are minimized by the roll-bond technology and by the planarity of one side of the heat exchange surface); 25 mm of polystyrene is used as rear absorber insulation. All of the system is included in an aluminium frame with an overall weight of 40–45 kg (Figure 4).
- PVTWIN – model 422 – manufactured by the PVTWINS (The Netherlands). It is a flat plate, glazed, liquid cooled collector, bought by the Department. The cells are a multi-crystalline type with a gross area of 2.54 m^2 (overall dimensions: 1.895 m × 1.895 m × 0.16 m) and nominal power of 295 W_p (open circuit voltage of 43 V, short circuit current of 9.3 A and electrical efficiency of 11.6 % at STC). The absorber is a plate-and-tube type made of copper: the absorber is properly glued to the rear part of the PV laminate and insulated with 40 mm of polyurethane. All the system is included in an aluminium frame with an overall weight of about 100 kg (Figure 5).
- MSS manufactured by the Millennium Electric T.O.U. (Israel). It is a flat plate, unglazed, liquid/air cooled collector, bought by the Department. The cells are a multi-crystalline type with a gross area of 2.7 m^2 (overall dimensions: 2.184 m × 1.270 m × 0.088 m) and nominal power of 300 W_p (open circuit voltage of 21.8 V, short circuit current of 19.2 A and electrical efficiency of 11.5% at STC). The absorber is a plate-and-tube type made of aluminium: pipes are all in parallel

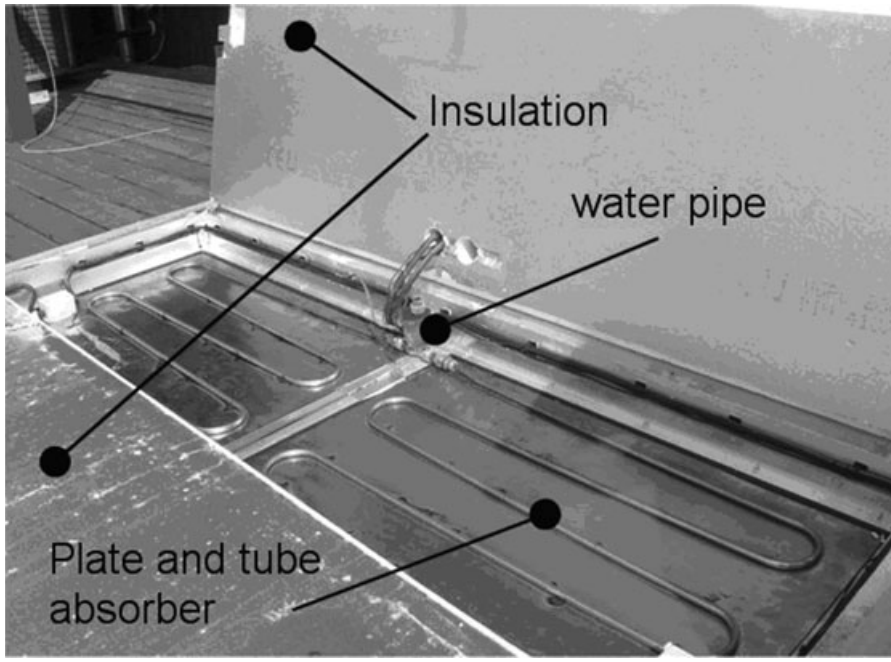

Figure 5. *PVTWIN: removed back side insulation with plate and tube absorber view.*

as described in Figure 6 together with air channels. Two headers are set in the shorter sides of the collector to direct the air from the inlet air duct to the collector air channels and from the collector air channels to the outlet air duct. All of the system is included in a stainless steel and back plastic frame with an overall weight of 80–100 kg (Figure 6).

The three collectors are set southward with a tilt angle of 30º (as to get the maximum annual energy for a latitude of 45º). A picture of the test rig is shown in Figure 7, whereas, the test rig scheme is depicted in Figure 8.

The test rig piping lines can be split into two circuits:

- The water storage tank circuit: the water storage is kept between 12ºC and 14ºC thanks to a 5 kW chiller. The chilled water before reaching the storage tank is sent to a plate heat exchanger via an automatic 3-way valve driven by a temperature controller, set to have a well defined collector circuit water temperature at the outlet of the heat exchanger (T_8).
- The collectors circuit: the water at the outlet of the plate heat exchanger gets to the header: here it is possible to send the water to the PVTWIN collector (Line 1) or/and to the COGEN/MSS collector (Line 2) and to partially by-pass the collectors through the by-pass line. As can be seen, only one collector between

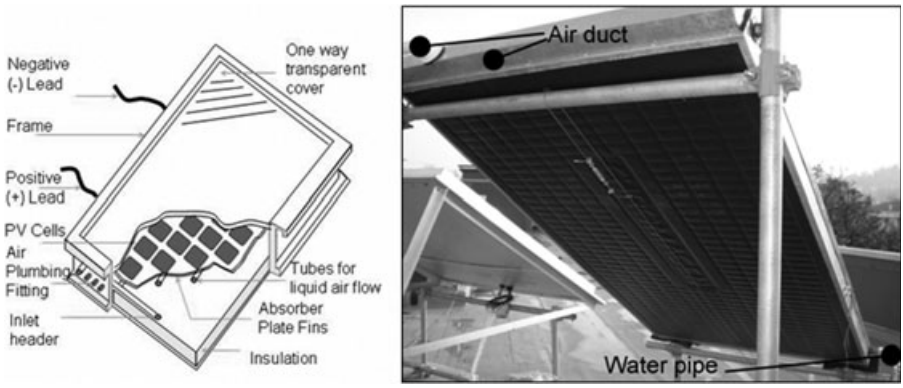

Figure 6. *MSS: schematic view (left) and rear side of the collector with indication of the inlet water pipe and outlet air duct (right).*

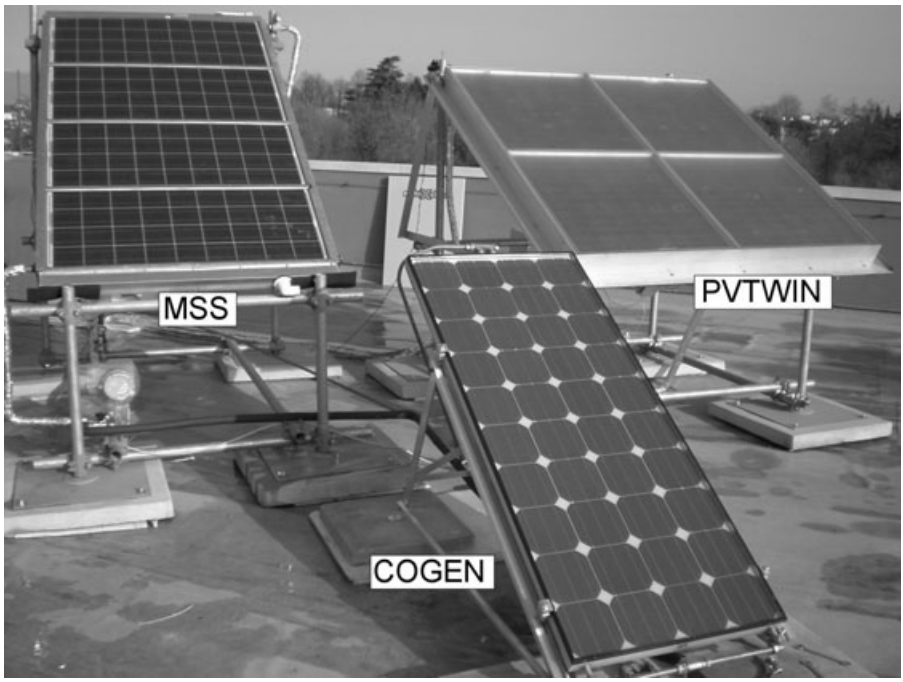

Figure 7. *Picture of the three PV/T collectors tested in the test rig.*

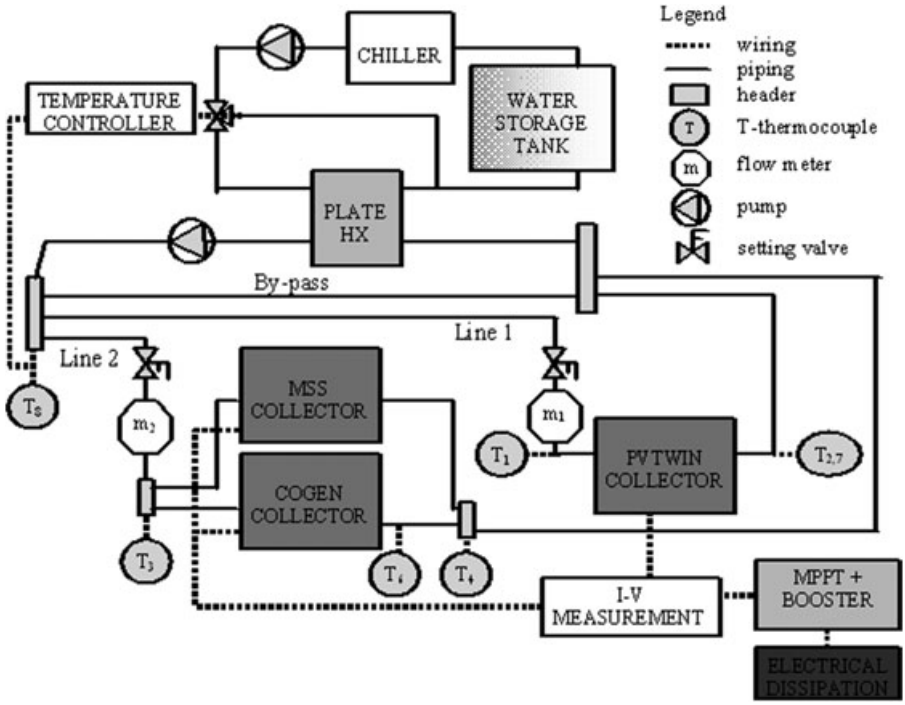

Figure 8. *Schematic of the PV/T collectors test rig.*

COGEN and MSS can be measured at once, because only one flow meter (m_2) is available for the Line 2. The mass flow rate can be set by the setting valve above the flow meter.

From the electrical point of view, each collector can be connected to the current-voltage measurement circuit to measure the electrical power produced by the collector. The electrical scheme of the measurement circuit is shown on the left-hand side of Figure 9: the three resistors R1, R2, R3 have 0.2 Ω, 10 kΩ, 100 kΩ of resistance respectively and are used to get voltage signals proportional to the current I (V_1) and voltage V (V_2) of the collector PV laminate, that is (Equation 34):

$$I = \frac{V_1}{R_1} \quad V = V_1 + V_2 \cdot \frac{R_2 + R_3}{R_2} \tag{34}$$

The R_4 resistor is the equivalent value of the dissipative resistances (it was chosen to totally dissipate the electrical energy since there were no possibilities to use it.).

The outside ambient conditions (solar radiation, ambient temperature) and mass flow rates are measured with the devices whose characteristics are depicted in [8].

The eight T-type thermocouples were periodically calibrated with a reference Pt100 thermometer to ensure the thermocouples had an error of 0.1ºC compared to the true value.

All the signals coming from the above described devices are acquired via a Field Point 2210 data logger (National Instruments) and monitored by an on-purpose software in LabView 7.1 environment.

5. PV/T measurements

The measurements took place on a series of sunny days with clear skies and different conditions with regard to the global solar radiation on the collector surface (two levels, 250 to 400 W m^{-2} and 690 to 800 W m^{-2}) and water mass flow rate (40, 80 and 120 kg h^{-1} m^{-2}). In order to get measurements not too much affected by thermal transient regime, each test had a duration of 15 to 20 minutes.

The first step was to define the electrical behaviour of the PV cells undertaking a flash test by manually varying the electrical load (equivalent dissipative resistances, R_4 in Figure 9) of the collector. Figure 10 and Figure 11 depict the voltage-power characteristics of the PVTWIN and the MSS collectors. Tests have been carried out at a specific mass flow rate of 80 kg h^{-1} m^{-2} (see [5] for hints about optimum mass flow rate) and at two levels of solar radiation (300 and 800 W m^{-2}) and water inlet temperature (20 and 30ºC).

The figures point out the voltage-current state for maximum DC electrical power in the vicinity of the curve knee; furthermore, increasing inlet water temperature has a negative effect on the electrical power produced by the collectors, in terms of 8%

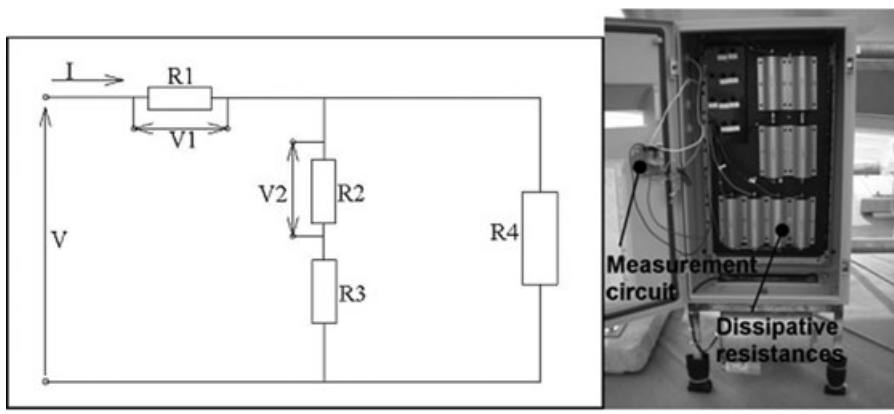

Figure 9. *Current/Voltage measurement circuit schematic (left) and picture showing both the measurement circuit and the dissipative resistances (right).*

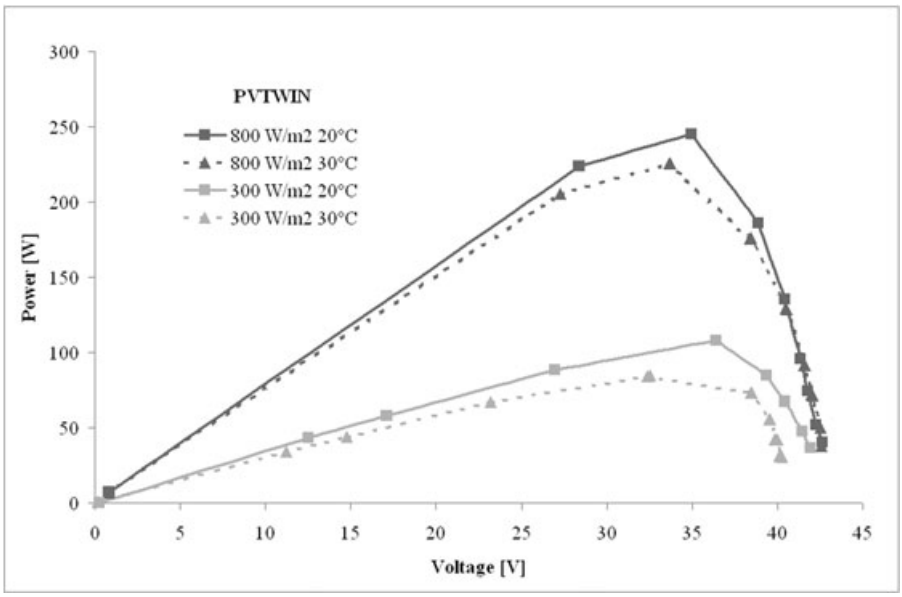

Figure 10. *Measured V-P curve for PVTWIN at 300 and 800 W m^{-2} of global solar radiation (respectively 23 and 28°C of ambient temperature), 20 and 30°C of inlet water temperature flowing through the collector.*

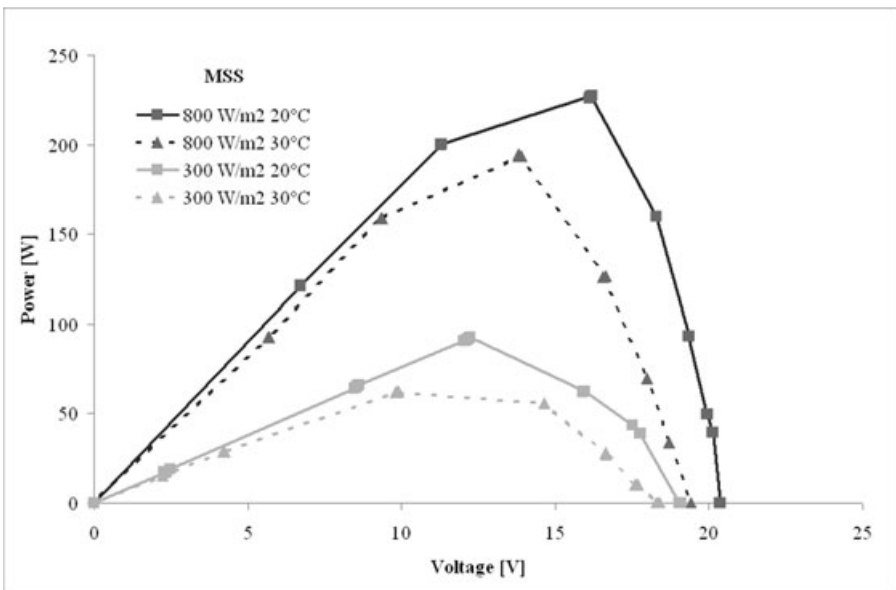

Figure 11. *Measured V-P curve for MSS at 300 and 800 W m^{-2} of global solar radiation (respectively 25 and 30°C of ambient temperature), 20 and 30°C of inlet water temperature flowing through the collector.*

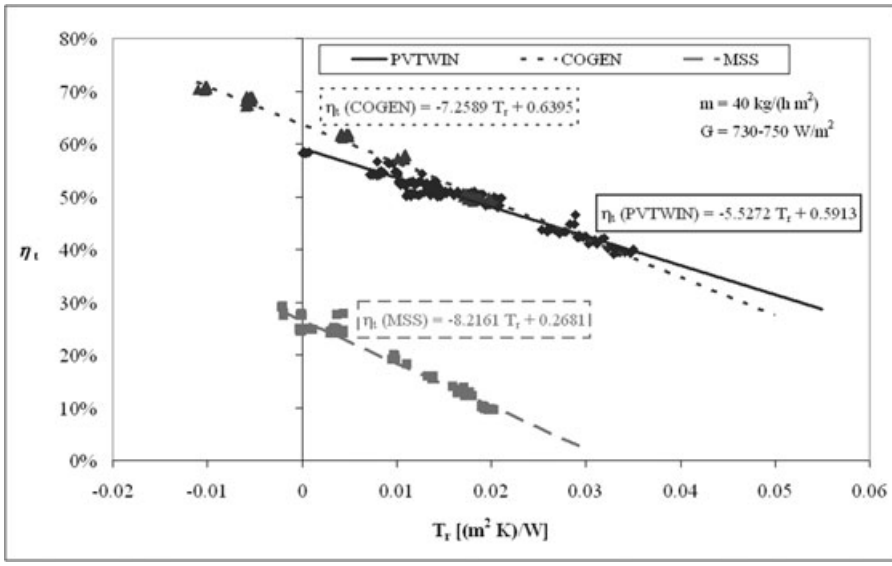

Figure 12. *Thermal efficiency of the three collectors at about 750 W m^{-2} of global solar radiation, 28ºC of ambient temperature, 40 kg h^{-1} m^{-2} water flow rate.*

and 19% respectively for 800 and 300 W m^{-2} solar radiation for PVTWIN collector (the same penalizations are 16% and 20% for MSS collector).

The COGEN collector has not been characterized under the V-I and V-P point of view, because of a technical problem: probably EVA layers damaged by the high stagnation temperature reached after a first period of measurements.

The following tests have been carried out to measure the efficiencies of the three collectors. Figure 12 to Figure 15 report only the main results, solar global radiation (G = 730 to 770 W m^{-2}) and at an ambient temperature of 28ºC. The thermal efficiency of the collector was measured as (Equation 35):

$$\eta_t = \frac{\dot{m} \cdot A_{coll} \cdot c_p \cdot (T_{out} - T_{in})}{G \cdot A_{coll}} \tag{35}$$

and the electrical efficiency (Equation 36):

$$\eta_e = \frac{V \cdot I}{G \cdot A_{coll}} \tag{36}$$

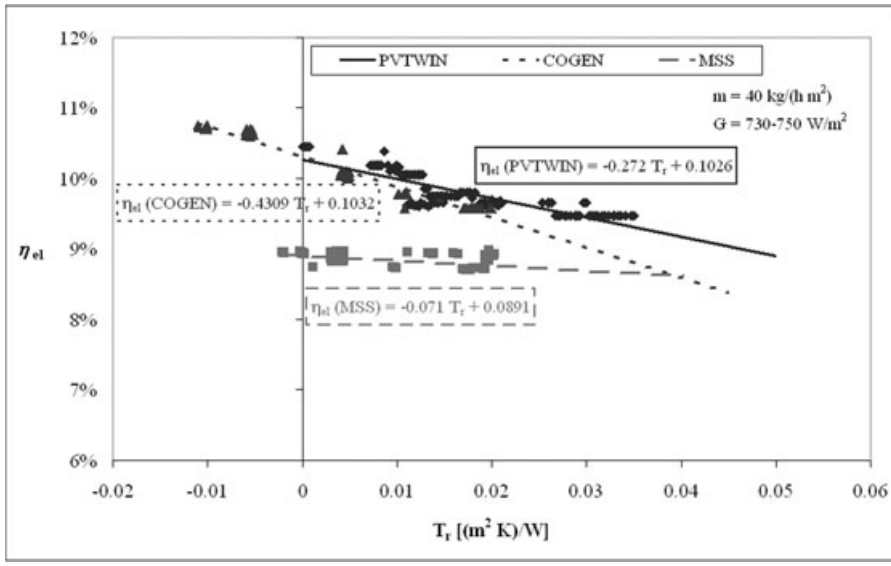

Figure 13. *Electrical efficiency of the three collectors at about 750 W m^{-2} of global solar radiation, 28°C of ambient temperature, 40 kg h^{-1} m^{-2} water flow rate.*

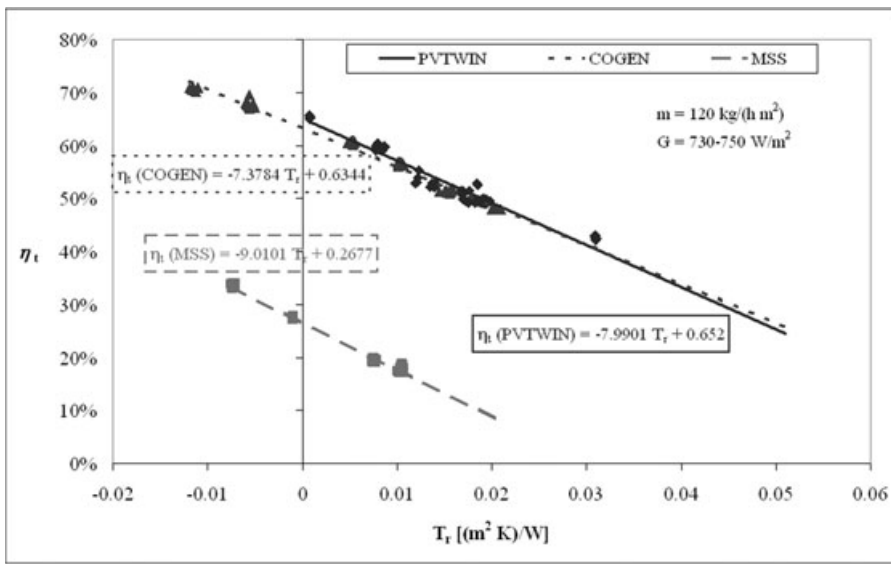

Figure 14. *Thermal efficiency of the three collectors at about 750 W m^{-2} of global solar radiation, 28°C of ambient temperature, 120 kg h^{-1} m^{-2} water flow rate.*

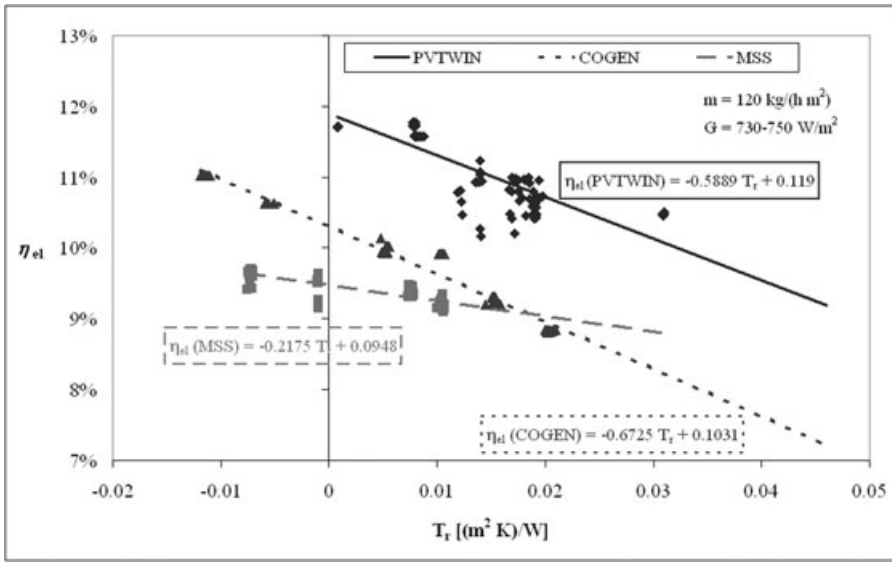

Figure 15. *Electrical efficiency of the three collectors at about 750 W m^{-2} of global solar radiation, 28ºC of ambient temperature, 120 kg h^{-1} m^{-2} water flow rate.*

Both the electrical and thermal efficiencies are plotted as a function of the reduced temperature T_{red} (Equation 37):

$$T_{red} = \frac{T_{avg} - T_{amb}}{G} \quad \text{where} \quad T_{avg} = \frac{T_{out} + T_{in}}{2} \tag{37}$$

Compared to the two other collectors, the MSS one is unglazed and can work with both water and air: that is, it has water inlet/outlet pipes and air inlet/outlet ducts. By the way, during our tests the air ducts were kept closed and only water was used to remove heat from the PV. The expected thermal efficiency is significantly less than that for a glazed type, mainly due to the frontal side thermal losses as described in the introduction part: at zero the reduced temperature thermal efficiency is 27%, decreasing more slowly with 40 instead of 120 kg h^{-1} m^{-2} water flow rate. Glazed type collectors show a better thermal efficiency, substantially equivalent for COGEN and PVTWIN; anyway, the latter is more penalized at a higher mass flow rate (slope increases more at higher mass flow rate). The water temperature increase in the collectors is in the range of 2 to 8ºC as a function of the mass flow rate.

With regard to electrical efficiency, the last two collectors have the best behaviour: at zero reduced temperature both have an electrical efficiency of 10.3% even if increasing abscissa (i.e. because surface collector temperature increases) PVTWIN efficiency is less sensitive (more constant). The latter remark is also true for the MSS collector (the slope is even lower than PVTWIN) and for all the collector types electrical efficiency decreases more quickly with a higher mass flow rate.

As already stated in former studies [9], it is interesting to evaluate the exergetic efficiency of the three PV/T collectors in the same conditions of Figure 12 to Figure 15.

It is well known that exergy is a state function representing the quota directly convertible in mechanical work of a quantity of energy. While electrical energy is basically pure exergy, thermal energy that cannot be converted in mechanical work without a temperature difference between source and sink, has an exergetic quota depending on such a temperature difference. So it is possible to define an exergetic efficiency of the PV/T panels, that is the ratio between useful exergy (in output) and used exergy (in input). In fact, Equations 38 are true:

$$\eta_{ex,t} = \frac{q_{ex}}{q} = \frac{\dot{m}[h_{out} - h_{in} - T_{amb}(s_{out} - s_{in})]}{\dot{m}c_p(T_{out} - T_{in})} \cong \frac{[(T_{out} - T_{in}) - T_{amb}\ln(T_{out}/T_{in})]}{(T_{out} - T_{in})}$$
$$= 1 - \frac{T_{amb}}{(T_{out} - T_{in})}\ln\frac{T_{out}}{T_{in}} \qquad (38)$$
$$\xi_{ex,e} = \eta_e \quad \xi_{ex,t} = \eta_t \cdot \eta_{ex,t} \quad \xi_{ex,tot} = \xi_{ex,e} + \xi_{ex,t}$$

where $\eta_{ex,t}$ is the exergetic quota of the useful thermal power produced by the collectors (varying in the range of 1 to 8%) and $\xi_{ex,e}$, $\xi_{ex,t}$, $\xi_{ex,tot}$ respectively the electrical, thermal and total exergetic efficiency (reference for exergy is the measured ambient (external) temperature, 28ºC). Exergetic efficiency of hybrid collectors is higher than PV only collectors (by the quantity $\eta_t \cdot \eta_{ex,t}$) and, above all, than thermal only collectors (by the quantity η_e). Figure 16 and Figure 17 depict the total exergetic efficiency of the three collectors for the two mass flow rates (40 and 120 kg h^{-1} m^{-2}), assuming the same values of Figure 12 to Figure 15 as regard solar radiation, inlet temperature and ambient temperature. The COGEN collector is the best for $T_{red} >$ 0.02 and $\dot{m} = 40$ kg h^{-1} m^{-2} but, while both MSS and PVTWIN show a better behaviour with higher mass flow rate, the COGEN collector decreases its performance at $\dot{m} = 120$ kg h^{-1} m^{-2}.

From all the measured data (not only the ones reported here) it is possible to make the following statements, that are quite in agreement with previous results [10]:

- with glazed collectors, when global solar radiation is high (700 to 800 W m^{-2}) it is advisable to use higher values of water mass flow rate, in order to guarantee an appropriate cooling of the PV laminate thus limiting the negative influence of temperature increase on PV performance;
- with unglazed collectors, conversely, lower mass flow rates are better in order not to penalize too much thermal efficiency;
- for the same reason, when global solar radiation is lower (350 to 400 W m^{-2}), for both glazed and unglazed technologies it is advisable to use lower mass flow rates;
- glazed collectors are preferable at latitudes with high annual global solar radiation, unglazed at latitudes with low annual global solar radiation;

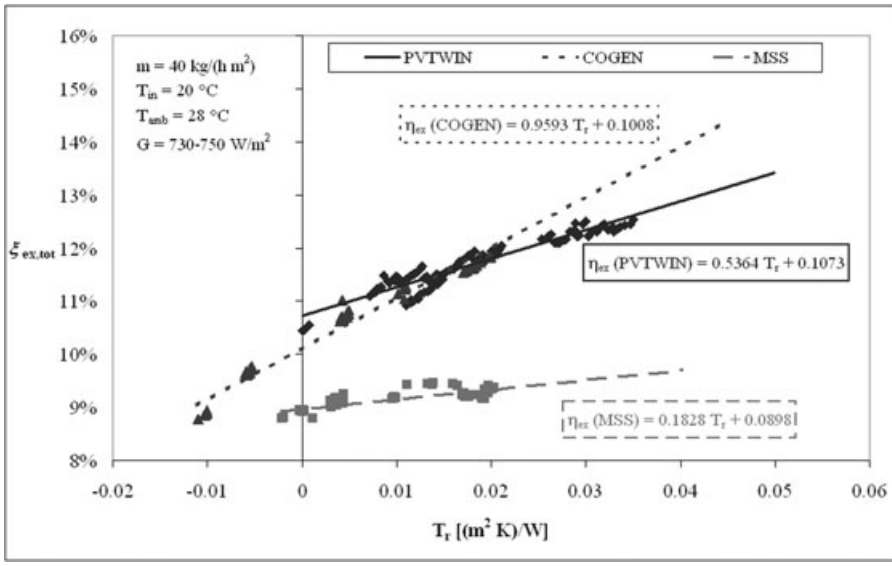

Figure 16. *Exergetic efficiency of the three collectors at about 750 W m^{-2} of global solar radiation, 28ºC of ambient temperature, 20ºC of inlet water temperature, 40 kg h^{-1} m^{-2} water flow rate.*

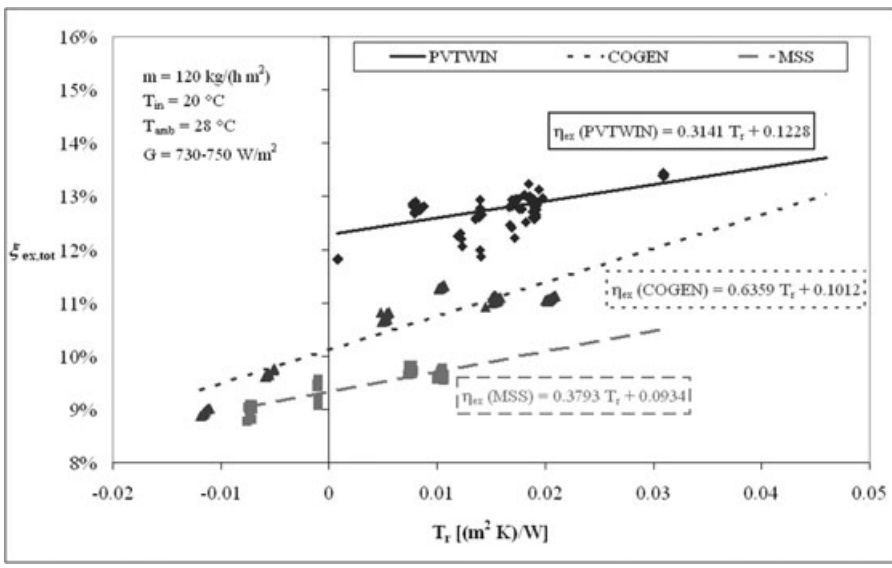

Figure 17. *Exergetic efficiency of the three collectors at about 750 W m^{-2} of global solar radiation, 28ºC of ambient temperature, 20ºC of inlet water temperature, 120 kg h^{-1} m^{-2} water flow rate.*

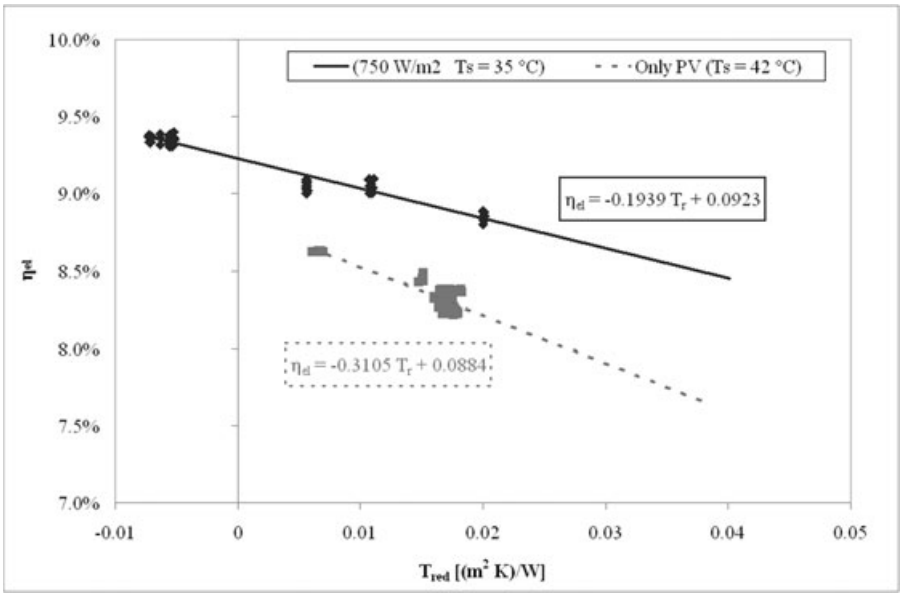

Figure 18. *Electrical efficiency of MSS collector at about 750 W m^{-2} of global solar radiation, 80 kg h^{-1} m^{-2} water flow rate, with and without thermal production.*

– cogeneration of thermal energy combined with electrical energy allows higher electrical efficiency of the collectors, even if such an increase is not extremely relevant. Figure 18 depicts the data measured on the MSS collector in terms of electrical efficiency, with and without thermal production: electrical efficiency increase is, in relative terms, of 4.5% at zero reduced temperature (something more at $T_{red} > 0$), that is 0.4% in absolute terms. Also, it is worth stressing that the real advantage of PV/T is the thermal production, against an improvement in electrical efficiency.

6. Conclusions

The main purpose of the test rig set-up at the Department of the University of Padova in Vicenza was to measure the thermal and electrical performances of a self-built PV/T glazed liquid cooled collector and to compare it with other state-of-the-art commercially available PV/T collectors. The experimental results are quite in agreement with calculated values by a simulation program based on a detailed analytical model.

The results show that the thermal efficiencies at a zero reduced temperature for the glazed type collectors (PVTWIN, COGEN) are comparable and around 60% with 10 to 12% of electrical efficiency; the thermal efficiency is expected to increase to around 70% for thermal energy only production. Water temperature increase in the collectors is in the range of 2 to 8ºC as a function of the mass flow rate. When

considering an unglazed water cooled PV/T collector, the thermal efficiency is supposed to drastically decrease to around 30% at a zero reduced temperature as a consequence of the frontal side collector thermal losses. By the way, a positive implication is better PV cells behaviour since the glass cover reflection is avoided and the average cells temperature is lower when considering the same boundary conditions.

Finally, a critical point for the glazed systems is the risk of high PV stagnation temperatures when no heat is removed from the collector during high solar radiation days.

References

[1] Ministry of Productive activities, DM 28/07/2005, Standards for the promotion of electric production by photovoltaic conversion of solar radiation (in Italian).
[2] Ministry of Economic development, DM 19/02/2007, Standards for the promotion of electric production by photovoltaic conversion of solar radiation, in accomplishment of article 7 of the act D.Lgs. 29th December 2003, n. 387 (in Italian).
[3] Italian Parliament, L 27/12/2006, n. 296, Financial act 2007 (in Italian).
[4] Italian Parliament, L 24/12/07, n. 244, Financial act 2008 (in Italian).
[5] Recoaro city, 2007, 'Photovoltaic cogeneration: development of components and system for the production of electric and thermal energy by solar radiation for residential, tertiary and industrial buildings', Final Report.
[6] Y. Tripanagnostopoulos, T. Nousia, M. Souliotis and P. Yianoulis, 2002, 'Hybrid Photovoltaic/Thermal Solar Systems', *Solar Energy*, 72(3) (2002), 217–234.
[7] M. Bazilian, F. Leenders, G. C. Van Der Ree and D. Prasad, 'Photovoltaic cogeneration in the built environment', *Solar Energy*, 71(1) (2001), 57–69.
[8] R. Lazzarin and L. Zamboni, 'Experimental analysis of photovoltaic cogeneration modules', *Proceedings of Climamed 2007*, 5th–7th September, Genova (Italy).
[9] T. Fujisawa and T. Tani, 'Annual exergy evaluation on photovoltaic-thermal hybrid collector', *Solar Energy Materials and Solar Cells*, 47 (1997), 135–148.
[10] H. A. Zondag, D. W. de Vries, W. G. J. van Helden, R. J. C. van Zolingen and A. A. van Steenhoven, 'The yield of different combined PV-thermal collector designs', *Solar Energy*, 74 (2003), 253–269.